Analysis of TM and TE Modes in Eccentric Coaxial Lines Based on Bipolar Coordinate System

Jun Zhou [1], Meiyan Chen [2], Renbin Zhong [1], and Shenggang Liu [1]

[1] Terahertz Research Center, School of Physical Electronics
University of Electronic Science and Technology of China, Chengdu, Sichuan 610054, China
zhoujun123@uestc.edu.cn, zhoujun@uestc.org

[2] Southwestern Institute of Physics, Chengdu, Sichuan 610041, China
mychen0014@126.com

Abstract ─ The cutoff wavenumbers, cutoff frequencies, field distributions and dispersive characteristics of TM and TE modes (higher order modes) in eccentric coaxial lines are carefully calculated by a new method directly based on the finite difference method (FDM) in bipolar coordinate system (BCS). Detailed comparisons with the previous results in the literature demonstrate the accuracy of the proposed method. Several characteristic features of the field distributions and the dispersion relations are also indicated. This method and its variations are very suitable and efficient for the computation of electromagnetic field problems in transmission lines with eccentric parallel cylinders.

Index Terms ─ Bipolar coordinate system, eccentric coaxial line, finite-difference method, transmission line, waveguide.

I. INTRODUCTION

The coaxial transmission lines have been widely used in different devices for various applications from the early 1900s. As a special case, the coaxial line with an eccentric inner conductor is termed as the eccentric coaxial line, which has been suggested to be used as an adjustable quarter-wave transformer for TEM mode propagation [1]. The effect of the displacement of the inner conductor on the electromagnetic characteristics of this kind of transmission lines was firstly investigated in 1960s [2]. As the eccentricity between the two conductors increases, higher order TM and TE modes may be excited at relatively high frequencies. For this problem, lots of methods mainly based on the conformal mapping and/or the boundary value approach have been reported in the literature continuously [2-11]. These methods have proven to be powerful for the solution of various wave-field problems. However, they are often found to be somewhat complex in practical applications. Analysis of TM and TE modes (higher order modes) in eccentric coaxial lines still remains interesting and challenging in the theory of electromagnetism.

The aim of this paper is to present a relatively simple method for the numerical analysis of eccentric coaxial lines through a computational approach. A new method which is directly based on the finite difference method (FDM) [12] in bipolar coordinate system (BCS) [13] is selected for much of this modeling effort. The FDM is a versatile and powerful technique for the computation of electromagnetic field problems, which is sufficient to allow us to investigate the higher order TM and TE modes in eccentric coaxial lines. The BCS has been successfully applied to the calculation of scattering from circular cylinders [14,15], which is much more convenient than the translational addition theorem of Bessel functions for transferring the fields component between two cylindrical coordinate systems [16].

This paper is organized as follows. We begin by discussing the methodology in Section II. The numerical results are then explored in detail and their comparisons with the previous results discussed in Section III. Finally, further discussion and conclusions are drawn in Section IV and Section V, respectively.

II. MODELING USING 2-D FDM IN BCS

A. Modeling in BCS

In uniform waveguides and transmission lines, the waveguiding structures are not changed along the propagating direction. The cross section of an eccentric coaxial line is shown in Fig. 1 (a). It contains a circular outer conductor and an eccentric circular inner conductor. The radii of the outer and inner circles are r_1 and r_2 respectively, and d is the distance between their centers.

This kind of waveguiding structure can be easily defined in the bipolar coordinate system (ξ, η, z) as shown in Fig. 1 (b) [13]. Let P_1 and P_2 be two fixed points in any z-plane with the coordinates (a, 0) and (-a, 0) respectively. The equations:

Submitted On: September 30, 2013
Accepted On: October 22, 2015

$$(x - a\coth\xi)^2 + y^2 = a^2\,\mathrm{csch}^2\,\xi, \quad (1)$$

$$x^2 + (y - a\cot\eta)^2 = a^2\csc^2\eta, \quad (2)$$

describe two families of orthogonal circles. Equation (1) describes the circles whose centers lie on the *x*-axis. The point P_1 at (a, 0) corresponds to $\xi = +\infty$, whereas its image P_2 at (-a, 0) corresponds to $\xi = -\infty$, and the *y*-axis is approached when $\xi = 0$. Equation (2) describes the circles whose centers lie on the *y*-axis and all of which pass through the fixed points P_1 and P_2. The parameter η is confined to the range $0 \le \eta \le 2\pi$. A value less than π is assigned to the arc above the *x*-axis, while the lower arc is denoted by a value of η equal to π plus the value of η assigned to the upper segment of the same circle.

The relation between BCS and Cartesian coordinate system can be described as:

$$x = h_1 \sinh\xi, \quad (3)$$

$$y = h_2 \sin\eta, \quad (4)$$

$$z = h_3 z, \quad (5)$$

where the metrical coefficients are:

$$h_1 = h_2 = \frac{a}{\cosh\xi - \cos\eta} = h,\ h_3 = 1. \quad (6)$$

Suppose the two circles in Fig. 1 (a) both lie to the right of the *y*-axis in Fig. 1 (b), as shown in Fig. 1 (c), the parameters stated above are related by the following equations:

$$d = a(\coth\xi_1 - \coth\xi_2), \quad (7)$$

$$r_1 = a\,\mathrm{csch}\,\xi_1, \quad (8)$$

$$r_2 = a\,\mathrm{csch}\,\xi_2. \quad (9)$$

Then, we can get the transformation relations:

$$a = \frac{\sqrt{\left[(r_1 + r_2)^2 - d^2\right]\left[(r_1 - r_2)^2 - d^2\right]}}{2d}, \quad (10)$$

$$\xi_1 = \mathrm{arcsinh}\frac{a}{r_1}, \quad (11)$$

$$\xi_2 = \mathrm{arcsinh}\frac{a}{r_2}. \quad (12)$$

Here, in order to define the entire region in BCS, the parameter ξ is confined to the range $\xi_1 \le \xi \le \xi_2$, in order to define the entire region in BCS together with the other confinement $0 \le \eta \le 2\pi$.

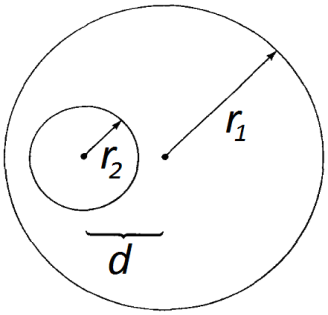

(a)

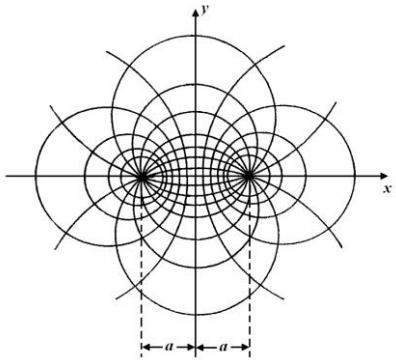

(b)

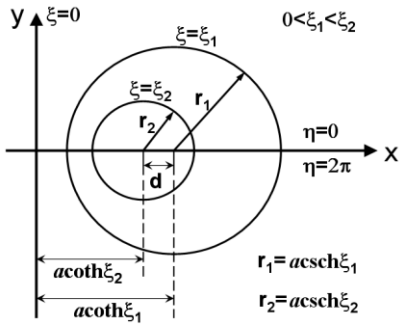

(c)

Fig. 1. Modeling in bipolar coordinate system: (a) cross section of eccentric coaxial line, (b) bipolar coordinate system, and (c) relations between the parameters.

B. Helmholtz equation and boundary conditions

Maxwell equations for the potential $\varphi(\xi, \eta, z)$ of an eccentric coaxial line lead to the following homogeneous Helmholtz equation in BCS:

$$\nabla_\perp^2\varphi + k_c^2\varphi = 0, \quad (13)$$

where $\nabla_\perp^2 = \frac{1}{h^2}\left(\frac{\partial^2}{\partial\xi^2} + \frac{\partial^2}{\partial\eta^2}\right)$, $k_c^2 = k^2 - k_z^2$, $k = \frac{\omega}{c}$, and c is the speed of light.

For TEM mode, $k = k_z$, when $\mathrm{ch}\xi - \cos\eta \ne 0$ we can get the Laplace equation:

$$\left(\frac{\partial^2}{\partial\xi^2} + \frac{\partial^2}{\partial\eta^2}\right)\varphi = 0, \quad (14)$$

which can be analytically solved by means of the variable separation approach.

For TM and TE modes, the Helmholtz equation is:

$$\frac{(\cosh\xi - \cos\eta)^2}{a^2}\left(\frac{\partial^2}{\partial\xi^2} + \frac{\partial^2}{\partial\eta^2}\right)\varphi + k_c^2\varphi = 0. \quad (15)$$

It has been proven strictly in mathematics that this equation can't be solved by means of the variable separation approach. Fortunately, this problem can be easily solved by means of the numerical methods such as the FDM and the finite element method (FEM).

For TM modes, $\varphi = E_z$, the Dirichlet boundary condition $\varphi = 0$ is employed on the boundaries $\xi = \xi_1$ and

$\xi = \xi_2$. While for TE modes, $\varphi = H_z$, the Neumann boundary condition $\partial\varphi/\partial n = 0$ is used. In addition, with consideration of the rotational symmetry, the periodic boundary conditions should be applied on the boundaries $\eta = 0$ and $\eta = 2\pi$.

C. FDM applied to the Helmholtz equation

According to Eq. (15), we can easily obtain the difference form of the Helmholtz equation in BCS on an orthogonal mesh. Based on the equation and the boundary conditions, a differentiation matrix A can be obtained for solving the eigenvalue problem:

$$A\Phi = k_c^2\Phi = \lambda\Phi, \tag{16}$$

where Φ is the eigenvector of φ values and $\lambda = k_c^2$ is the required eigenvalue.

Finally, the cutoff wavenumbers, the cutoff frequencies, the field distributions and the dispersive characteristics can all be achieved from the solution of this eigenvalue problem.

III. NUMERICAL RESULTS

Based on the above methodology, a special code has been constructed using the Microsoft Visual C++ programming language. The aim of this code is to solve the eigenvalue problems in BCS, print and save numerical results, and plot the field distributions. This code is very fast, it takes less than half a minute to calculate the first twenty eigenvalues for each case listed in the tables below on a single personal computer.

According to the previous publications, in order to be convenient for comparison and conversion, the results are always given for an outer circle of unit radius, the radius of the inner circle being denoted $\alpha = r_2 / r_1$ and the distance between the centers of the circles denoted $\beta = d / r_1$. To convert these frequencies to those of a similar region with outer circle of radius r_1, divide these frequencies by r_1. When comparing the results of other authors, their frequencies were normalized to an outer circle of radius 1. In this case, the transformation relations demonstrated in Eqs. (10)-(12) can be rewritten as:

$$a = \frac{\sqrt{\left[(1+\alpha)^2 - \beta^2\right]\left[(1-\alpha)^2 - \beta^2\right]}}{2\beta}, \tag{17}$$

$$\xi_1 = \operatorname{arcsinh} a, \tag{18}$$

$$\xi_2 = \operatorname{arcsinh} \frac{a}{\alpha}. \tag{19}$$

In our calculations, the values of α and β for which Kuttler [3] presented tables are selected. The main parameters used in the present calculations are summarized in Table 1. For purposes of direct comparisons, the cutoff wavenumbers obtained by the present calculations together with those evaluated by Kuttler [3], Vishen [4], Zhang [6] and Das [9] for symmetric and asymmetric TM as well as TE modes are given in Tables 2 to 5.

Table 1: Main parameters for the calculations

Parameters	Values
r_1	1
r_2	The value of α
d	The value of β
Range of ξ	Calculated from Eqs. (17)-(19)
Range of η	$[0, 2\pi]$
$\Delta\xi$	0.01
$\Delta\eta$	0.01

From the tables we can find that for TM modes, our results coincide with those of Vishen [4] and Zhang [6], which are all within the bounds reported by Kuttler [3]. For TE modes, our results do not agree with those of [4,6] very well, but most of them are within the bounds reported by Kuttler, and are all very close to the upper bounds. Obviously, for both TM and TE modes, our results do not agree with those of Das [9], we think the main reason is that the small numbers of the grid nodes (corresponding to the large spatial steps) used in [9] cause rough mesh and low precision in their calculations.

Then, based on the cutoff wavenumbers listed in the tables, the eigenvalues and the corresponding eigenvectors in Eq. (16) can be easily achieved from the relation $\lambda = k_c^2$. After that, the field distributions can be directly plotted using the φ values in the eigenvectors and the mode numbers can be easily determined from the field distribution plots. In Fig. 2 and Fig. 3, we detail the field distributions of the longitudinal field components for the lowest TM and TE modes corresponding to the case of $\alpha = 0.5$ and $\beta = 0.2$, respectively. Here, we use the prefix "e" for even (symmetric) modes and "o" for odd (asymmetric) modes [2,17].

Finally, the cutoff angular frequencies ω_c, the cutoff frequencies f_c and the dispersive characteristics can be easily achieved from the relations $\omega_c = 2\pi f_c = f_c c$, $\omega^2 = \omega_c^2 + k_z^2 c^2$. The cutoff frequencies for the lowest TM and TE modes corresponding to the case of $\alpha = 0.5$ and $\beta = 0.2$ are given in Table 6, and the dispersion curves for these modes are shown in Fig. 4.

From the field distributions and the dispersion curves we can find several characteristic features: (1) each of the TE_{mn} and TM_{mn} modes splits up into one even mode and one odd mode when $m \neq 0$; (2) the TM_{0n} modes are all even modes, and the TE_{0n} modes do not exist; (3) the cutoff frequencies of the TE_{mn} modes are much lower than those of the TM_{mn} modes with the same mode numbers m and n; (4) the cutoff frequencies of the eTE_{mn} modes and the oTE_{mn} modes with the same mode numbers are very close to each other, so their dispersion curves nearly overlap.

Table 2: Cutoff wavenumbers for symmetric TM modes

Case	Our Results	Das [9]	Zhang [6]	Vishen [4]	Kuttler Bounds [3]	
					Lower	Upper
α=0.5 β=0.1	5.4695	5.432	5.46953	5.4695	5.46911	5.47043
	6.4747	6.431	6.47472	6.4747	6.47403	6.47547
	7.3062	7.257	7.30617	7.3062	7.30527	7.30683
	7.8692	7.815	7.86924	7.8692	7.86823	7.86982
	8.4965	8.433	8.49647	8.4965	8.495	8.4972
α=0.5 β=0.2	4.8106	4.792	4.8106	4.8106	4.80935	4.81191
	6.1724	6.127	6.1724	6.1724	6.1703	6.1735
	7.3945	7.386	7.3945	7.3945	7.3907	7.3957
	8.4974	8.445	8.4974	8.4974	8.4894	8.4991
	9.3409	9.158	9.3409	9.3409	9.2694	9.3488
α=0.5 β=0.3	4.3071	4.293	4.3071	4.3071	4.3042	4.3118
	5.8903	5.828	5.8903	5.8903	5.8736	5.8944
	7.3197	7.198	7.3197	7.3197	7.24	7.325
	8.2909	7.953	8.2909	8.2909	8.081	8.316
	8.6388	8.365	8.6388	8.6388	8.382	8.646
α=2/3 β=0.2	6.2399	6.217	6.2399	6.2399	6.2379	6.242
	7.6769	7.65	7.6769	7.6769	7.6728	7.6787
	9.0439	8.99	9.0439	9.0439	9.0323	9.0456
	10.3535	10.309	10.3534	10.3536	10.318	10.356
	11.6134	11.523	11.6134	11.6184	11.539	11.616
α=0.25 β=0.25	3.4723	3.446	3.4723	3.4723	3.4687	3.4752
	4.9221	4.897	4.9221	4.9221	4.911	4.9249
	5.9268	5.862	5.9268	5.9268	5.893	5.93
	6.7154	6.58	6.7154	6.7154	6.591	6.723
	6.7527	6.626	6.7527	6.7527	6.622	6.767
α=0.25 β=0.5	2.9824	2.981	2.9824	2.9824	2.887	2.996
	4.7868	4.781	4.7868	4.7868	4.088	4.827
	5.8084	5.777	5.8084	5.8084	-	5.877
	6.2439	6.234	6.2439	6.2439	-	6.323
	7.5586	7.356	7.5586	7.5592	-	7.735

Table 3: Cutoff wavenumbers for asymmetric TM modes

Case	Our Results	Das [9]	Zhang [6]	Vishen [4]	Kuttler Bounds [3]	
					Lower	Upper
α=0.5 β=0.1	5.9918	5.953	5.99176	5.9918	5.99121	5.99257
	6.9203	6.878	6.92031	6.9203	6.91953	6.92102
	7.7123	7.619	7.71232	7.7123	7.7113	7.71299
	8.4845	8.371	8.4845	8.4845	8.483	8.4852
	9.3564	9.204	9.3564	9.3564	9.3542	9.3572
α=0.5 β=0.2	5.5114	5.485	5.5114	5.5114	5.5098	5.5125
	6.7991	6.729	6.7991	6.7991	6.7964	6.8002
	7.9607	7.931	7.9607	7.9607	7.9559	7.9619
	9.0091	8.897	9.0091	9.0091	8.9996	9.0106
	9.9556	-	9.9556	9.9556	9.9316	9.9577
α=0.5 β=0.3	5.1224	5.088	5.1224	5.1222	5.1179	5.1257
	6.621	6.563	6.621	6.621	6.5994	6.6251
	7.991	7.839	7.991	7.991	7.876	7.997
	9.1877	8.814	9.1877	9.1877	8.829	9.21
	9.2676	8.975	9.2676	9.2676	8.9	9.276
α=2/3 β=0.2	6.9683	6.887	6.9683	6.9683	6.9654	6.9702
	8.3682	8.347	8.3682	8.3682	8.3631	8.37
	9.7053	9.61	9.7053	9.7053	9.6922	9.7071
	10.9892	10.932	10.9892	10.9892	10.947	10.992
	12.2266	-	12.2266	12.2266	12.128	12.229
α=0.25 β=0.25	4.264	4.248	4.264	4.264	4.2583	4.268
	5.5393	5.488	5.5393	5.5393	5.5239	5.5425
	6.6357	6.552	6.6357	6.6357	6.582	6.641
	7.7135	7.46	7.7135	7.7135	7.443	7.723
	7.7243	-	7.7243	7.7243	7.488	7.735
α=0.25 β=0.5	4.0338	3.973	4.0338	4.0338	3.858	4.043
	5.5432	5.494	5.5432	5.5432	4.58	5.575
	6.9144	6.914	6.9144	6.9144	-	6.992
	7.156	7.144	7.156	7.156	-	7.208
	8.1858	-	8.1858	8.1858	-	8.355

Table 4: Cutoff wavenumbers for symmetric TE modes

Case	Our Results	Das [9]	Zhang [6]	Vishen [4]	Kuttler Bounds [3]	
					Lower	Upper
α=2/3 β=0.2	1.322	1.318	1.3222	1.2522	1.32027	1.32221
	2.4458	2.422	2.4445	2.4365	2.4408	2.4446
	3.6216	3.565	3.6217	3.6209	3.6157	3.6218
	4.7881	4.672	4.7897	4.7897	4.7804	4.7901
	5.9378	5.717	5.9378	5.9379	5.9218	5.9385
α=0.475 β=0.315	1.5195	-	1.5158	1.4407	1.5132	1.5159
	2.7341	-	2.7343	2.7256	2.727	2.7345
	3.9275	-	3.9237	3.924	3.8978	3.9248
	4.3704	-	4.4035	-	4.342	4.407
	5.0806	-	5.0801	5.0799	4.977	5.084
α=1/3 β=2/9	1.5808	1.569	1.5806	1.5619	1.5766	1.5807
	2.9063	2.863	2.9065	2.9064	2.8968	2.9067
	4.1164	4.016	4.1152	4.1152	4.0944	4.1161
	4.2334	4.56	4.2342	4.422	4.2146	4.2356
	5.2649	5.083	5.2673	5.2669	5.219	5.27
α=0.5 β=0.2	1.4076	1.401	1.40792	1.3793	1.40694	1.40793
	2.6863	2.659	2.6861	2.6849	2.6837	2.6862
	3.9296	3.918	3.9295	3.9295	3.9247	3.9298
	5.0178	4.872	5.0175	-	4.9937	5.0192
	5.1135	5.512	5.1133	5.1131	5.1031	5.1139
α=0.25 β=0.25	1.6848	1.633	1.681	1.665	1.6768	1.6811
	2.9616	2.908	2.9679	2.9678	2.9445	2.9684
	3.9744	3.899	3.9861	-	3.939	3.988
	4.145	4.352	4.165	4.1191	4.105	4.168
	5.2913	5.055	5.2946	5.2942	5.111	5.303
α= 0.15875 β=0.379	1.8089	-	1.7944	1.7769	1.7603	1.7948
	3.0013	-	2.9992	2.9932	2.871	3.004
	3.7523	-	3.7703	3.8632	3.432	3.775
	4.1806	-	4.1824	4.1808	3.76	4.21

Table 5: Cutoff wavenumbers for asymmetric TE modes

Case	Our Results	Das [9]	Zhang [6]	Vishen [4]	Kuttler Bounds [3]	
					Lower	Upper
α=2/3 β=0.2	1.1928	1.189	1.19175	1.1917	1.19001	1.19176
	2.4297	2.418	2.4304	2.4307	2.4267	2.4305
	3.6196	3.415	3.6202	3.6203	3.6142	3.6203
	4.7879	4.669	4.7896	4.7896	4.7804	4.7899
	5.9324	-	5.9379	5.9379	5.9231	5.9385
α=0.475 β=0.315	1.3783	-	1.3741	1.374	1.3715	1.3741
	2.7257	-	2.7196	2.7187	2.7125	2.7198
	3.9152	-	3.9237	3.9244	3.9069	3.9247
	5.0657	-	5.0793	5.0796	5.041	5.083
	5.4061	-	5.4232	5.3686	5.325	5.427
α=1/3 β=2/9	1.5461	1.532	1.5435	1.5435	1.5393	1.5436
	2.9063	2.863	2.9064	2.9058	2.8966	2.9067
	4.1164	4.016	4.1152	4.1152	4.0955	4.1161
	5.1588	5.053	5.1651	5.1606	5.131	5.167
	5.2705	-	5.2758	5.2758	5.237	5.279
α=0.5 β=0.2	1.3522	1.344	1.35218	1.3522	1.35114	1.35219
	2.6843	2.657	2.6834	2.6838	2.6815	2.684
	3.9268	3.892	3.9295	3.9296	3.9247	3.9298
	5.1128	4.982	5.1131	5.1131	5.1036	5.1138
	5.8274	-	5.8315	5.8106	5.793	5.834
α=0.25 β=0.25	1.6458	1.633	1.6489	1.649	1.6446	1.649
	2.9671	2.915	2.9678	2.9667	2.9547	2.9682
	4.145	3.972	4.1581	4.1579	4.12	4.16
	5.0636	4.654	5.0581	5.0616	4.978	5.06
	5.3089	-	5.2964	5.2965	5.175	5.302
α= 0.15875 β=0.379	1.7544	-	1.7583	1.7584	1.733	1.7584
	2.9884	-	2.9879	2.9848	2.873	2.989
	4.164	-	4.1614	4.159	3.78	4.17

Table 6: Cutoff frequencies for the lowest TM and TE modes with $\alpha = 0.5$ and $\beta = 0.2$

Modes		k_c	ω_c ($\times 10^9$)	f_c (GHz)
TM modes	eTM_{01}	4.8106	1.4432	0.2297
	oTM_{11}	5.5114	1.6534	0.2631
	eTM_{11}	6.1724	1.8517	0.2947
	oTM_{21}	6.7991	2.0397	0.3246
	eTM_{21}	7.3945	2.2184	0.3531
	oTM_{31}	7.9607	2.3882	0.3801
TE modes	oTE_{11}	1.3522	0.4057	0.06457
	eTE_{11}	1.4076	0.4223	0.06721
	oTE_{21}	2.6843	0.8053	0.1282
	eTE_{21}	2.6863	0.8059	0.1283
	oTE_{31}	3.9268	1.178	0.1875
	eTE_{31}	3.9296	1.1789	0.1876

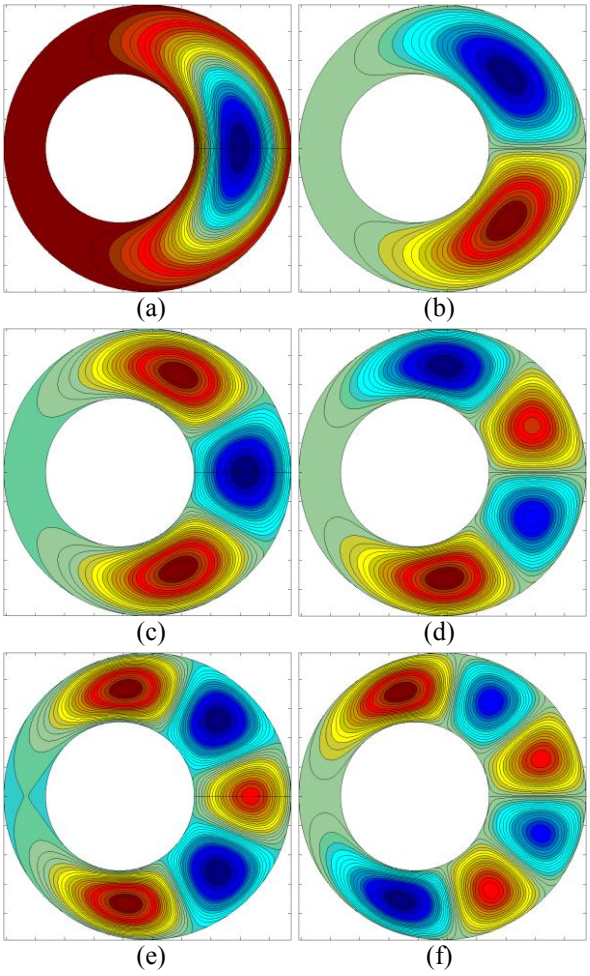

Fig. 2. Field distributions of E_z for the lowest TM modes with $\alpha = 0.5$ and $\beta = 0.2$: (a) eTM_{01} mode, (b) oTM_{11} mode, (c) eTM_{11} mode, (d) oTM_{21} mode, (e) eTM_{21} mode, and (f) oTM_{31} mode.

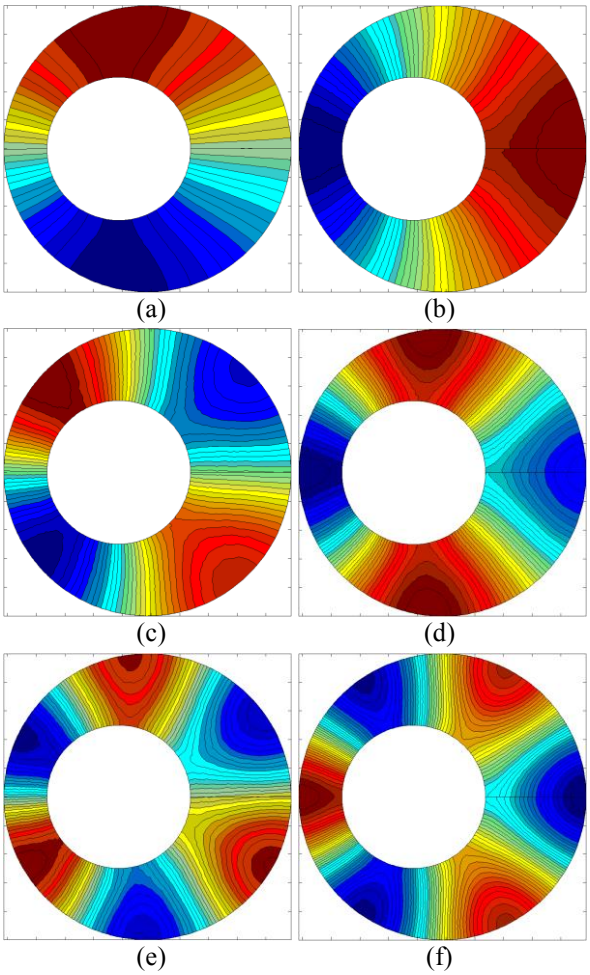

Fig. 3. Field distributions of H_z for the lowest TE modes with $\alpha = 0.5$ and $\beta = 0.2$: (a) oTE_{11} mode, (b) eTE_{11} mode, (c) oTE_{21} mode, (d) eTE_{21} mode, (e) oTE_{31} mode, and (f) eTE_{31} mode.

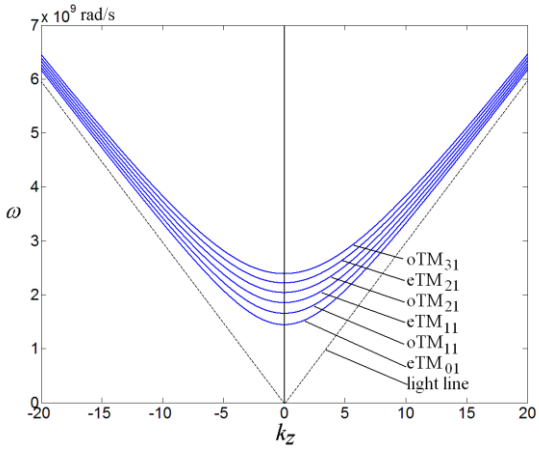

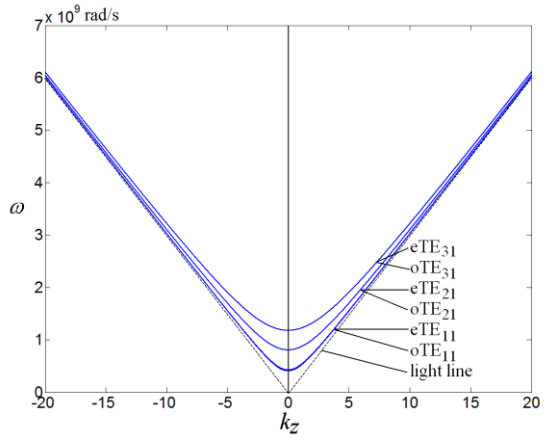

(b)

Fig. 4. Dispersion curves for the lowest TM and TE modes with α = 0.5 and β = 0.2: (a) TM modes, and (b) TE modes.

The dependence of the cutoff frequency on the eccentricity of the coaxial line has been intensively analyzed in the literature, so we will not discuss here. The deviation between the numerical results calculated by the present method and those presented in the literature is very small. This agreement justifies the validity of the present analysis. Because BCS is very suitable for transmission lines with eccentric parallel cylinders, the success of the present method encourages its use for other problems, such as the analysis of lunar waveguides mentioned in [3] and two-wire waveguides [18,19]. For these problems, only some variations of the boundary conditions in the present method are required.

IV. DISCUSSION

A. Accuracy and convergence rate

It is necessary to discuss the characteristics of the proposed method. Here, we will discuss the accuracy and convergence rate, which are two of the most essential characteristics of a numerical method.

The accuracy obtained by the proposed method is mainly due to the easy definition of eccentric coaxial waveguiding structure in BCS. Given an arbitrary cross section of an eccentric coaxial line, we can easily get the required parameters in BCS through the transformation relations demonstrated in Eqs. (10)-(12). Since the inner and outer boundaries are all parallel to the ξ-axis in BCS, there is no need to worry about the errors from the saw-tooth shaped boundaries, which has long been suffered by the FDM in other coordinate systems, as shown in Fig. 5.

From the Taylor series of $\varphi_{i,j}$ in BCS, we obtain:

$$\frac{\partial^2 \varphi_{i,j}}{\partial \xi^2} = \frac{\varphi_{i+1,j} - 2\varphi_{i,j} + \varphi_{i-1,j}}{(\Delta\xi)^2} + O\left[(\Delta\xi)^2\right], \qquad (20)$$

$$\frac{\partial^2 \varphi_{i,j}}{\partial \eta^2} = \frac{\varphi_{i,j+1} - 2\varphi_{i,j} + \varphi_{i,j-1}}{(\Delta\eta)^2} + O\left[(\Delta\eta)^2\right], \qquad (21)$$

which indicate that the second derivative of $\varphi_{i,j}$ is second-order accurate. So, in the case of $\Delta\xi = \Delta\eta = 0.01$ we used for the calculations, an accuracy of 0.0001 can be achieved. Even higher accuracy can also be easily achieved by reducing the spatial step size.

In order to solve the eigenvalue problem demonstrated in Eq. (16) with high efficiency, the Arnoldi method has been adopted for the fast computations. The Arnoldi method is well known for solving large matrix eigenvalue problems. For this classical method, the convergence rate has been intensively analyzed in the publications in mathematics [20,21], so we will not analyze it any more.

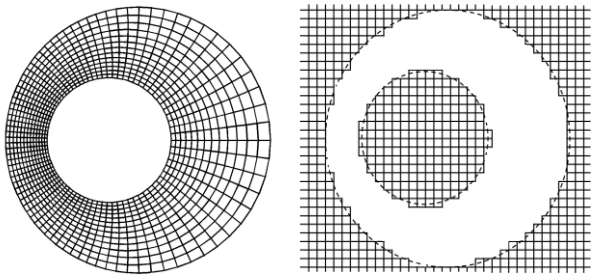

(a) (b)

Fig. 5. Comparison of meshes in different coordinate systems: (a) mesh with smooth boundaries in BCS, (b) and mesh with saw-tooth shaped boundaries in Cartesian coordinate system.

B. Comparisons with other methods

Among all the numerical methods, the FDM is the oldest and also the simplest. Its simplicity, however, makes it very robust and efficient [12]. It is essential to compare the proposed method with other commonly used numerical methods. Here, we will give the comparisons among the FDM, the finite difference time-domain (FDTD) method, the FEM method and the method of moments (MoM).

The FDM used in this paper is a numerical procedure for converting partial differential equations (PDEs) of a boundary-value problem into a set of algebraic equations to obtain approximate solutions, it is very suitable and efficient for the problem analyzed here. The method has been widely used in a variety of engineering fields. For a practical problem, if the coordinate system is properly chosen, the saw-tooth shaped boundaries can be well avoided and the degree of accuracy can reach a very high level, which has just been discussed.

The applications of FDM to the analysis of electromagnetic problems was empowered by the development of a unique scheme for the discretization of

the time-domain Maxwell's equations, which is known today as the FDTD method. With the further development, the FDTD became probably the most popular numerical technique for solving complex electromagnetic problems [12]. But, the FDTD is well suited to time-domain full-wave analysis. There is no need to solve the eigenvalue problems using the FDTD method.

Like the FDM, the FEM is a numerical procedure to convert partial differential equations into a set of linear algebraic equations to obtain approximate solutions. Instead of approximating the differential operators, the FEM approximates the solution of a partial differential equation. Today, the FEM is recognized as a general preeminent method applicable to a wide variety of engineering and mathematical problems [12]. Generally, when compared with the FDM, the FEM has better accuracy and stability, but its realization is too complicated. Furthermore, it requires larger computer memory and longer computation time.

The MoM, also known as the moment method, is another powerful numerical technique in electromagnetics. Like the FEM, the MoM transforms the governing equation of a boundary-value problem into a matrix equation to enable its solution on digital computers. Today, it has become one of the most predominant methods in computational electromagnetics [12]. But the MoM is particularly well suited to open-region electromagnetic problems such as wave scattering and antenna radiation, and its realization is also too complicated when compared with the FDM.

To conclude, according to the above comparisons, it is easy to see that the FDM in BCS used in this paper is the most convenient, efficient and straightforward numerical method with high simplicity and practicality for the analysis of TM and TE modes in eccentric coaxial lines and other transmission lines with eccentric parallel cylinders.

V. CONCLUSION

A new method directly based on the FDM in BCS is developed, which is very suitable and efficient for calculating TM and TE modes in eccentric coaxial lines. Making use of this method, the cutoff wavenumbers, cutoff frequencies, field distributions and dispersive characteristics of higher order TM and TE modes in eccentric coaxial lines are given. Our results agree well with the previous results in the literature. In addition, several characteristic features of the field distributions and the dispersion relations are also indicated.

The accuracy of this method is mainly due to the easy definition of eccentric coaxial waveguiding structure in BCS. Furthermore, some variations of this method can be applied to the computation of electromagnetic field problems in other transmission lines with eccentric parallel cylinders (connected or not), such as lunar waveguides, two-wire waveguides, and so on.

ACKNOWLEDGMENT

Jun Zhou wishes to express his sincere thanks to Prof. Zhaoyun Duan, Prof. Wei Shao and Prof. Shengjian Lai in School of Physical Electronics of UESTC for their kind help and comments. This work was supported by the Natural Science Foundation of China under Grant No. 61505022.

REFERENCES

[1] P. Grivet, *Physics of Transmission Line at High and Very High Frequency*, Academic Press, London, 1970.

[2] H. Y. Yee and N. F. Audeh, "Cutoff frequencies of eccentric waveguides," *IEEE Trans. Microwave Theory Tech.*, vol. 14, no. 10, pp. 487-493, Oct. 1966.

[3] J. R. Kuttler, "A new method for calculating TE and TM cutoff frequencies of uniform waveguides with lunar or eccentric annular cross section," *IEEE Trans. Microwave Theory Tech.*, vol. 32, no. 4, pp. 348-354, Apr. 1984.

[4] A. Vishen, G. P. Srivastava, G. S. Singh, and F. Gardiol, "Calculation of cutoff wavenumbers for TE and TM modes in tubular lines with offset center conductors," *IEEE Trans. Microwave Theory Tech.*, vol. 34, no. 2, pp. 292-294, Feb. 1986.

[5] M. Davidovitz and Y. T. Lo, "Cutoff wavenumbers and modes for annular-cross-section waveguide with eccentric inner conductor of small radius," *IEEE Trans. Microwave Theory Tech.*, vol. 35, no. 5, pp. 510-515, May 1987.

[6] L. Zhang, J. Zhang, and W. Wang, "Correct determination of TE and TM cutoff wavenumbers in transmission lines with circular outer conductors and eccentric circular inner conductors," *IEEE Trans. Microwave Theory Tech.*, vol. 39, no. 8, pp. 1416-1420, Aug. 1991.

[7] A. A. Kishk, R. P. Parrikar, and A. Z. Elsherbeni, "Electromagnetic scattering from an eccentric multilayered circular cylinder," *IEEE Trans. Antennas Propag*., vol. 40, no. 3, pp. 295-303, Mar. 1992.

[8] B. N. Das and O. J. Vargheese, "Analysis of dominant and higher order modes for transmission lines using parallel cylinders," *IEEE Trans. Microwave Theory Tech.*, vol. 42, no. 4, pp. 681-683, Apr. 1994.

[9] B. N. Das and S. B. Chakrabarty, "Evaluation of cut-off frequencies of higher order modes in eccentric coaxial line," *IEE Proc. - Microwave Antennas Propag*., vol. 142, no. 4, pp. 350-356, Aug. 1995.

[10] X. Zhou, Z. Yu, and W. Lin, "Characteristics of eccentric coaxial line using conformal mapping and finite-difference time-domain method,"

Microwave and Optical Tech. Lett., vol. 16, no. 11, pp. 249-252, Nov. 1997.

[11] S. B. Chakrabarty, S. B. Sharma, and B. N. Das, "Higher-order modes in circular eccentric waveguides," *Electromagnetics*, vol. 29, no. 5, pp. 377-383, 2009.

[12] J. M. Jin, *Theory and Computation of Electromagnetic Fields*, John Wiley & Sons, Inc., New Jersey, 2010.

[13] J. A. Stratton, *Electromagnetic Theory*, McGraw-Hill, New York, 1941.

[14] J. M. Jarem, "Rigorous coupled wave analysis of bipolar cylindrical systems: scattering from inhomogeneous dielectric material, eccentric, composite circular cylinders," *Progress in Electromagnetics Research*, vol. 43, pp. 181-237, 2003.

[15] R. Herschmann and O. Büchel, "Radiation characteristics of a coaxial waveguide with eccentric inner conductor for application in hyperthermia and microwave reflex therapy," *Advances in Radio Science*, vol. 5, pp. 189-195, 2007.

[16] H. A. Yousif and A. Z. Elsherbeni, "Oblique incidence scattering from two eccentric cylinders," *Journal of Electromagnetic Waves and Applications*, vol. 11, no. 9, pp. 1273-1288, 1997.

[17] E. Abaka and W. Baier, "TE and TM modes in transmission lines with circular outer conductor and eccentric circular inner conductor," *Elec. Lett.*, vol. 5, no. 11, pp. 251-252, May 1969.

[18] H. Pahlevaninezhad, T. E. Darcie, and B. Heshmat, "Two-wire waveguide for terahertz," *Opt. Expr.*, vol. 18, no. 7, pp. 7415-7420, Mar. 2010.

[19] R. Zhong, J. Zhou, W. Liu, and S. Liu, "Theoretical investigation of a terahertz transmission line in bipolar coordinate system," *Science China Information Sciences*, vol. 55, no. 1, pp. 35-42, Jan. 2012.

[20] Y. Saad, *Numerical Methods for Large Eigenvalue Problems*, SIAM, Philadelphia, 1992.

[21] G. H. Golub and C. F. Van Loan, *Matrix Computations*, Third edition, The Johns Hopkins University Press, 1996.

Jun Zhou was born in Hubei Province, China, in 1980. He received the B.S. degree in Applied Physics and the Ph.D. degree in Plasma Physics from the University of Electronic Science and Technology of China (UESTC), Chengdu, China, in 2003 and 2009, respectively.

From October 2008 to May 2009, he was a Visiting Student in Queen Mary, University of London, UK. In 2009, he joined the faculty of UESTC. He is currently engaged in research in the Terahertz Science and Technology Research Center at UESTC in the areas of terahertz sources, terahertz spectroscopy and imaging, terahertz transmission lines and antennas, and computational electromagnetics.

Meiyan Chen was born in Shandong Province, China, in 1981. She received the B.S. degree in Applied Physics from the Liaocheng University, Liaocheng, China, in 2004, the M.S. degree in Condensed Matter Physics from the University of Electronic Science and Technology of China (UESTC), Chengdu, China, in 2007 and the Ph.D. degree in Nuclear Energy Technology and Development from the Southwestern Institute of Physics (SWIP), Chengdu, China, in 2012.

She is currently with the SWIP. Her research interests include theory, simulation and experimental works on novel materials and components.

Renbin Zhong was born in Jiangxi Province, China, in 1973. She received the M.S. degree in Optics from the Southwest Jiaotong University, Chengdu, China, in 2003 and the Ph.D. degree in Plasma Physics from the University of Electronic Science and Technology of China (UESTC), Chengdu, China, in 2012.

She is currently with the Terahertz Science and Technology Research Center, UESTC. Her research interests include terahertz sources, terahertz transmission and related components.

Shenggang Liu received the B.S. degree from the Southeast University (formerly Nanjing Polytechnic Institute), Nanjing, China, in 1995 and the Ph.D. degree in Physical Electronics from the University of Electronic Science and Technology of China (UESTC), Chengdu, China, in 1958.

Since 1964, he has been leading various research projects on gyrotrons, free electron lasers, and plasma electronics. He was a Distinguished Visiting Professor with Old Dominion University, Norfolk, VA, and the College of William and Mary, Williamsburg, VA, where he worked in the field of microhollow cathode discharges, microwave plasma excited excimer lasers, and electromagnetic field effect on biological cells. In 1980, he was elected Academician of the Chinese Academy of Sciences. In 1984, he was appointed Vice-President of UESTC and then served as President from 1986 to 2001. He is a Member of International Organizing Committee of IRMMW-THz Conferences, K. J. Button Prize Committee, et al. He serves as the Chair of the International Committee of SICAST Conferences. He is currently Professor and Director of the Terahertz Science and Technology Research Center, UESTC. His research interests include terahertz physics, microwave electronics, relativistic electronics, free electron laser, optics, and plasma physic.